Physics – Uspekhi **57** (11) 1118 – 1129 (2014)

INSTRUMENTS AND METHODS OF INVESTIGATION PACS numbers: **28.41.–i**, **28.65.+a**, 29.25.Dz, 52.55.Fa, 52.55.Jd

Hybrid systems for transuranic waste transmutation in nuclear power reactors: state of the art and future prospects

D V Yurov, V V Prikhod'ko

DOI: 10.3367/UFNe.0184.201411f.1237

Contents

Abstract. The features of subcritical hybrid systems (HSs) are discussed in the context of burning up transuranic wastes from the U–Pu nuclear fuel cycle. The advantages of HSs over conventional atomic reactors are considered, and fuel cycle closure alternatives using HSs and fast neutron reactors are comparatively evaluated. The advantages and disadvantages of two HS types with neutron sources (NSs) of widely different natures — nuclear spallation in a heavy target by protons and nuclear fusion in magnetically confined plasma — are discussed in detail. The strengths and weaknesses of HSs are examined, and demand for them for closing the U–Pu nuclear fuel cycle is assessed.

1. Introduction

Although the nuclear energy industry considerably contributes at present to the global production of electric power, it manifests a number of serious drawbacks. First, a disadvantage consists in the low utilization efficiency of nuclear raw material. In modern thermal atomic power plants only 5% of the enriched uranium undergoes fission in one manner or another, but, recalculated with respect to natural uranium, it is actually only about 1%. With account of modern consumption volumes of uranium, explored uranium ore deposits contain reserves for approximately 50 years [1] [1]. Second, the waste intended for long-term burial exhibits a long period of high radiotoxicity. The largest contribution to such activity during the time period of $10^3 - 10^5$ years is due to long-lived transuranic elements accumulated as a result of fuel irradiation. Such elements include plutonium and minor actinides (MAs), the main elements among the latter being neptunium, americium, and curium. The high radiotoxicity period of 10^5 years gives rise to difficulties related to the reliability of a long-term waste isolation from the ambient environment.

The above-specified shortcomings can be eliminated by closure of the nuclear fuel cycle (NFC) and active utilization of breeder reactors, i.e., by involving in the NFC transuranic elements which are presently practically unused. Then, plutonium can be effectively produced by fast reactors (FRs) in breeding mode of operation and further used as fuel.

At the same time, enrichment of fuel with minor actinides leads to a reduction in the delayed neutron effective fraction and to undesirable reactivity effects. Therefore, burning MAs up with the aid of conventional reactors may give rise to difficulties.

To resolve the problem described, besides commissioning fourth-generation reactors which offer in some way or another the acceptable decision, it is also possible to make use of so-called hybrid systems (HSs). An HS nuclear assembly, unlike conventional nuclear installations, is subcritical. For sustaining the chain reaction, an external neutron source (NS) of one construction or another is introduced into the HS. At present, those HSs that involve neutron sources based on nuclear spallation of heavy atoms exposed to a high-energy proton beam give rise to more interest. At the same time, in the past decade more and more popularity has been

D V Yurov, V V Prikhod'ko Budker Institute of Nuclear Physics, Siberian Branch of the Russian Academy of Sciences, prosp. Akademika Lavrent'eva 11, 630090 Novosibirsk, Russian Federation;
Nuclear Safety Institute, Russian Academy of Sciences, ul. Bol'shaya Tul'skaya 52, 115191 Moscow, Russian Federation;
Novosibirsk State University, ul. Pirogova 2, 630090 Novosibirsk, Russian Federation
E-mail: D.V.Yurov@inp.nsk.su; V.V.Prikhodko@inp.nsk.su

Received 18 December 2013, revised 12 August 2014
Uspekhi Fizicheskikh Nauk **184** (11) 1237 – 1248 (2014)
DOI: 10.3367/UFNr.0184.201411f.1237
Translated by G Pontecorvo; edited by A Radzig

[1] We mean resources with the cost of mining inferior to \$ 80 per kg of U_3O_8. If the cost is considered to be less than \$ 130 per kg, then the time required for exhaustion of the resources will be estimated to increase to 83 years.

gained by HS projects with thermonuclear NSs, which in the ideal case are capable of providing a significantly higher power of neutron production and a higher generation efficiency normalized to 1 W of spent power from the electrical supply network.

In principle, HSs can be used to resolve the following tasks of modern nuclear power engineering:

- the burning up of long-lived transuranic elements from spent nuclear fuel;
- the transmutation of radioactive fission products;
- the production of fuel isotopes for U–Pu and U–Th NFCs.

Such tasks can, naturally, be combined with the production of electric power.

In this article, HS projects are considered that are aimed at closure of the U–Pu NFC, i.e., at solving the first of the aforementioned tasks. The article outline is as follows. Section 2 deals with the influence of minor actinides on the behavior of the reactor core, which is precisely the reason for interest in HSs for the burning up of NFC transuranic waste. Section 3 describes closure scenarios for the U–Pu NFC involving the exploitation of HSs. Peculiarities of modern HSs with accelerator-driven NSs are dealt with in Section 4, and with thermonuclear NSs in Section 5. Issues of HS competitiveness are considered in Section 6. In the closing Section 7, general conclusions are made concerning the current state of affairs with HS studies and prospects for the burning up of transuranic elements.

2. Influence of minor actinides on the neutron kinetics of a reactor

The utilization of fuel with a high concentration of minor actinides in conventional reactors gives rise to difficulties related to the deterioration of core parameters affecting the safety and controllability of a reactor. We shall only deal qualitatively with the effects caused by MA addition to nuclear fuel. The main negative effects are the following [2, 3]:

- a reduction in the delayed neutron effective fraction;
- a positive reactivity gain due to a hardening of the neutron energy spectrum;
- a weakening of Doppler feedback coupling related to a change in the fuel temperature.

In the case of normal functioning, the reactor period $\tau = P/(\mathrm{d}P/\mathrm{d}t)$ (where P is the thermal power) is determined by the fraction of delayed neutrons and their contribution to successive acts of fissioning. Generally speaking, the emission energy spectra of prompt and delayed neutrons differ from each other (maximum emission of delayed neutrons occurs at the energy $E_{\mathrm{delayed}} \approx 0.5$ MeV, while in the case of prompt neutrons at the energy $E_{\mathrm{prompt}} \approx 1.5-2$ MeV). Therefore, the probability of leakage beyond the reactor core boundaries and the interaction cross sections of delayed neutrons with matter will also differ from the respective parameters for prompt neutrons. This difference is reflected in the effective fraction of delayed neutrons β_{eff}, which takes into account the importance of delayed neutrons, as opposed to that of prompt ones.

A number of minor actinides (for example, ^{237}Np, ^{241}Am, and ^{243}Am) possess small fission cross sections in the range of interaction energies below 0.1 MeV and relatively large cross sections of radiative neutron capture (Figs 1, 2). This leads to the effective absorption of delayed neutrons in reactions with MAs and to a lesser contribution from delayed neutrons to fission reactions, i.e., to a reduction in β_{eff}. At the same time, the fission cross sections in the high-energy region remain high and the contribution from prompt neutrons to the fission reactions is not reduced.

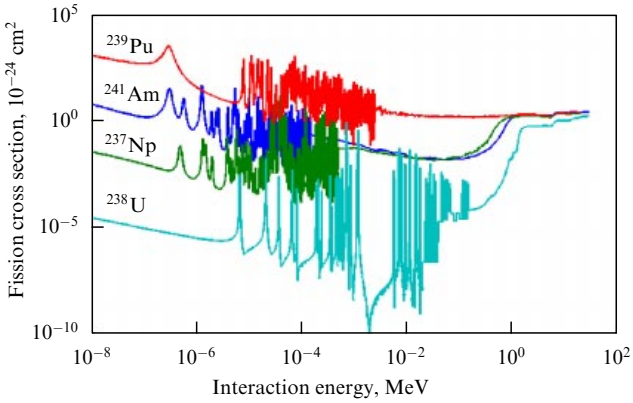

Figure 1. (Color online.) Fission cross sections of ^{241}Am, ^{237}Np versus energy of interaction with neutrons. The fission cross sections of ^{238}U and ^{239}Pu are presented for comparison. (Taken from data of Ref. [4].)

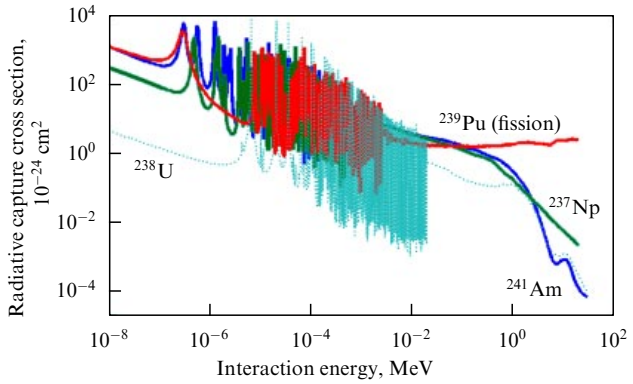

Figure 2. (Color online.) Cross sections of neutron radiative capture for ^{241}Am, ^{237}Np versus interaction energy. The capture cross section for ^{238}U and the ^{239}Pu fission cross section are presented for comparison. (Taken from data of Ref. [4].)

The energy dependence of the fission cross sections of the main MAs also determines the positive reactivity gain $\Delta\rho$ in the case of a hardening of the neutron energy spectrum, accompanying a decrease in the density of the coolant [2] with pronounced moderating properties (for example, of sodium [3]). As seen from Fig. 1, the MA fission cross sections undergo a sharp increase in the range of neutron energies of $10^{-1}-10^{0}$ MeV. Owing to a decrease in the heat carrier density, the neutron spectrum is shifted toward the region of higher energies, which leads to an enhancement of the fission reaction intensity and makes a positive contribution to the reactivity, $\Delta\rho > 0$.

Finally, weakening of the Doppler feedback coupling associated with a change in the fuel temperature is explained by the large cross sections of radiative neutron capture on a number of MAs within the interaction energy range of 10–100 keV being superior to the neutron capture cross section

[2] In principle, boiling of the coolant or its loss from the core can be interpreted as the reduction of density.

[3] Although sodium is utilized in fast neutron reactors, its moderating properties are sufficient for manifestation of the effect discussed.

Table 1. Influence of the fuel composition of a fast neutron reactor with a sodium heat carrier and oxide fuel on the parameters of the reactor assembly* [5].

Fuel composition	β_{eff}/β ($10^{-3}\%/10^{-3}\%$)	$T_{\text{fuel}}(\partial\rho/\partial T_{\text{fuel}})$, 10^{-3} %	$\Delta k/\Delta T_{\text{Na}}$, $10^{-3}\%$ K^{-1}
$(U_{0.8}, Pu_{0.2})\,O_2$	342/399	−810	+1.07
$(U_{0.5}, Pu_{0.2}, Am_{0.3})\,O_2$	204/307	−20	+1.79
$(Pu_{0.2}, Zr_{0.8})O_2$	206/221	−420	+0.72
$(Pu_{0.2}, Am_{0.3}, Zr_{0.5})\,O_2$	143/213	−20	+2.02

* In calculations, a model of an infinite regular lattice of fuel rods with hexagonal structure cells was used; $\Delta T_{\text{Na}} = 900\text{ K} - 700\text{ K}$.

on ^{238}U. An increase in temperature leads to a broadening of the resonances in the neutron interaction cross sections with core materials due to the Doppler effect (the Doppler effect is especially important for low-energy resonances). This effect manifests itself most rapidly when the fuel temperature changes. In conventional reactors, the condition $\partial\rho/\partial T_{\text{fuel}} < 0$ is fulfilled owing to low-energy resonances of the capture cross section on ^{238}U. Effective neutron absorption by minor actinides in the energy region of 10–100 keV leads to a smaller part of the delayed neutrons achieving low energies and, thus, the reactivity effect is weakened.

The example of how an MA added to the fuel affects the parameters of an FR with a liquid-metal heat carrier and oxide fuel is presented in Table 1.

All the above effects are reflected in a negative manner in the kinetics of reactors with an enhanced MA content in the fuel. Nevertheless, their influence can be reduced in the following ways:

- by enriching the fuel with ^{235}U for increasing the β_{eff} value;
- by using heat carriers with a small macroscopic neutron interaction cross section (lead,[4] gaseous heat carriers He, CO_2);
- by optimizing the reactor assembly to enhance the reactivity effects related to the leakage of neutrons from the reactor core;
- by allocating MAs in irradiation targets separately from the main fuel.

On the whole, from the point of view of neutron kinetics, the task of burning up MAs can be performed with the aid of conventional reactors and, to date, numerous critical burner projects have been developed. The assumed rate for burning up minor actinides differs greatly from one project to another, starting from ≈ 3 kg per TW of thermal (t) power per hour (kg (TW$^{(t)}$ h)$^{-1}$) [6] up to 10 kg (TW$^{(t)}$ h)$^{-1}$ according to the specific concept [7]. For comparison, the production of minor actinides by a standard pressurized water thermal reactor with fuel burnup depth of 60 GW day t^{-1} varies from 1.2 kg (TW$^{(t)}$ h)$^{-1}$ (if UO_2 fuel is used) to 4.1 kg (TW$^{(t)}$ h)$^{-1}$ [with Mixed OXide (MOX) fuel] [8].

Within the framework of the problem of NFC closure, hybrid systems exhibit one essential difference from conventional reactors. A doubtless advantage of HS consists in the fact that, when the power and efficiency of the neutron source are sufficiently high, the neutron multiplication factor can be determined from the system's safety requirements. Then, the maximum admissible addition to HS reactivity can be defined as

$$\Delta\rho_{\max} \approx \frac{1 - k_{\text{sub}}}{k_{\text{sub}}} + \beta_{\text{eff}} \gg \beta_{\text{eff}}\,, \tag{1}$$

where k_{sub} is the neutron multiplication factor in the subcritical assembly. Relation (1) signifies that, if $(1 - k_{\text{sub}})/k_{\text{sub}} \gg \beta_{\text{eff}}$, the controllability of a subcritical assembly depends weakly on the relative amount of delayed neutrons. Thus, choosing $k_{\text{sub}} = 0.95$, we arrive at $\Delta\rho_{\max} \approx 0.053$, which exceeds any value of β_{eff} from Table 1 by more than an order of magnitude.

From the above, it follows that in an HS it is possible to use such nuclear fuel that is little suited to be utilized in conventional reactors for safety reasons. A perfect case from the point of view of burning up MAs consists in the use of a fuel with an inert matrix and high MA enrichment, in which stable elements are substituted for ^{238}U; an example can be represented by a composite fuel such as CERCER (CERamic-CERamic) $(Pu, MA)O_2 + MgO$ or CERMET (CERamic-METal) $(Pu, MA)O_2 + Mo$ [9]. In this case, the possibility appears to achieve an MA burnup rate close to the highest possible achievable value[5] of ≈ 45 kg (TW$^{(t)}$ h)$^{-1}$. For example, in the system EFIT (European Facility for Industrial-scale Transmutation) (see Section 4 and Refs [10, 11]) the MA burnup rate to be expected amounts to 42 kg (TW$^{(t)}$ h)$^{-1}$.

3. Closure scenarios of the U–Pu nuclear fuel cycle

Since the beginning of the 2000s, a series of scrupulous investigations of possible scenarios of NFC closure taking advantage of existing or planned reactor installations has been performed. Particularly, a comparison was carried out of a number of scenarios of the total U–Pu NFC closure using dedicated burners, light-water reactors with MOX fuel, and fast-neutron reactors [12, 13]. Total closure implies utilization in the cycle of both uranium and plutonium isotopes and minor actinides, which would result in a reduction of the necessary isolation time of spent fuel in long-term repositories to ~ 500 years (when the characteristic isolation time is determined by the decay time of the radiological waste toxicity in the repository down to the toxicity level of the amount of nuclear raw material required for the production of 1 t of natural uranium). It must be noted that even in total closure scenarios a significant reduction of the necessary isolation time can only be achieved under the condition of a high decontamination level of the fission products sent to long-term repositories from admixtures of transuranic elements in the process of isotope separation [14]. On the whole, two fundamental conclusions can be drawn from the results of the aforementioned studies:

(1) HS burners for NFC closure will be in demand if the relative number of FRs is small in the reactor stock.

(2) Utilization of a subcritical MA burner will require development of methods for pyrometallurgical fuel reprocessing, since the existing methods for fuel processing [such as

[4] The natural mixture of lead isotopes exhibits a large cross section of inelastic interaction with neutrons at energies of > 0.5 MeV. The use of a lead heat carrier enriched with ^{208}Pb ensures that the influence of its density on the neutron energy distribution becomes smaller (see Ref. [2]).

[5] Assuming all the acts of fission take place in minor actinides with atomic mass $M_A \approx 240$ g mol^{-1} and the energy release in the case of a single fissioning nucleus to be $E \approx 200$ MeV, one can obtain the estimate indicated.

Table 2. Parameters of different NFC closure schemes. For comparison, we present characteristics of the open fuel cycle [13].

Scheme number	Fuel cycle	Composition of reactor stock	Relative cost of electric power when the price of natural uranium is \$ 50 per kg	Relative consumption of natural uranium	Volume of highly active waste for burial in geological formations: actinides/fission products kg $(TW^{(1)}h)^{-1}$**
1	Open fuel cycle	100% of thermal reactors with UO_2 fuel	1	1	1920/130
2	Closed cycle with burning of plutonium and MAs in FRs	63.2% of thermal reactors with UO_2 fuel, 36.8% of FR burners	1.09	0.63	1.68/118
3	Closed cycle with HS for burning MAs	66% of thermal reactors with UO_2 fuel, 9.8% of thermal reactors with MOX fuel, 19% of FRs with MOX fuel, 5.2% of ADS MA burners*	1.11	0.65	1.85/118
4	Closed cycle with HS for burning transuranic elements	75.1% of thermal reactors with UO_2 fuel, 9.4% of thermal reactors with MOX fuel, 15.5% of ADS burners of transuranic elements	1.2	0.76	2.0/122
5	Closed cycle with fuel reproduction in FRs	100% FR	1.2	0.004	0.76/86

* ADS — Accelerator-Driven System (see Section 4).
** Superscript (e) on TW points to electric power.

the PUREX process (Plutonium-Uranium Recovery by EXtraction)] are of little use for work with fuel exhibiting high thermal and neutron activities.

Table 2 presents the parameters of a number of NFC closure schemes based on the data of Ref. [13]. All the schemes presented concern the stationary conditions of electric power production and fuel mass flows. One can see that the scheme being the best from the point of view of efficient usage of natural resources and at the same time producing the least possible volume of highly active waste is the one involving fuel reproduction in FRs[6] (scheme 5). However, the latter requires gradual substitution of fast reactors for thermal reactors. For an extensive use of plutonium as the main fissionable element, its breeding is necessary; therefore, passage to such an NFC scheme will require some time. Moreover, NFCs involving extensive use of thermal reactors in the conditions of current prices for fuel material are cheaper, and the technology of thermal reactors long ago reached the stage of commercialization.[7] Therefore, the scheme of a closed NFC with fuel reproduction in FRs can be considered for now a target for the long-run perspective.

Although schemes 2–4 of NFC closure do not lead to any significant decrease in the consumption of fuel material, they permit significantly reducing the volume of highly active waste. These schemes are directed toward burning up plutonium, which cannot be considered effective utilization of the resources, taking into account the possibility of plutonium breeding; nevertheless, schemes 2–4 are of interest within a near-term perspective, since their implementation will require less time and their cost, in the case of schemes 2 and 3, will be lower than for the scheme 5. The advantages of HS burners can be most fully realized in the scheme 3, since it implies the use of uranium and plutonium isotopes in critical reactors with fuel based on uranium oxide (Uranium OXide, UOX) and MOX fuel, while only the burning up of the minor actinides (Fig. 3) will be performed by the hybrids, which permits the maximization of the burnup rate of MAs. Scheme 4 can be considered a method for NFC closure in conditions when conventional FRs are excluded from consideration. As is seen from Table 2, the cost of electric power, the consumption of raw materials, and the amount of highly active waste in the case of schemes 2 and 3 are practically identical, while the relative number of FRs in the reactor stock is lower in scheme 3.

Thus, the conclusion can be made that the higher the relative number of FRs among the available reactors, the lower the demand for HS burners of transuranic elements.

A disadvantage of the scheme 3 is the necessity of developing pyrometallurgical technology for the extraction of nuclear fuel isotopes, an alternative to the presently applied 'wet' extraction technologies [12, 13]. This is related to the high radiation activity of fuel for HS burners of minor actinides and to the radiolysis of organic compounds employed in the purex process (for example, tributyl phosphate) due to the action of α-particles.[8] Moreover, the standard purex recovery process does not imply separation of the minor actinides and lanthanides, a number of which have very large radiative neutron capture cross sections (in particular, Sm, Gd, Eu). Contrariwise, the pyrometallurgical extraction technology is based on the electrolysis of salts, and no use of organic compounds in it is intended; therefore, it is less sensitive to the high activity of the spent fuel from an HS MA burner.

[6] In the case of schemes 2–4, irradiated enriched uranium is considered a fuel material for FRs in the long-run perspective, instead of a waste to be buried within geological formations.

[7] It should be noted that within the framework of the NFC closure problem, it is also possible to examine a scheme with extended fuel breeding in FRs that involves thermal reactors. For such a scheme, however, it is necessary that the number of FRs with a breeding factor of > 1 is dominant in the reactor stock.

[8] For comparison, we can present residual heat release values peculiar to spent nuclear fuel (SNF) after the stage of intermediate storage. In a thermal reactor with UOX fuel, the heat release due to α-activity amounts to 0.5 W kg^{-1} of actinides, while in the case of an HS MA burner, it increases to 435 W kg^{-1} [12].

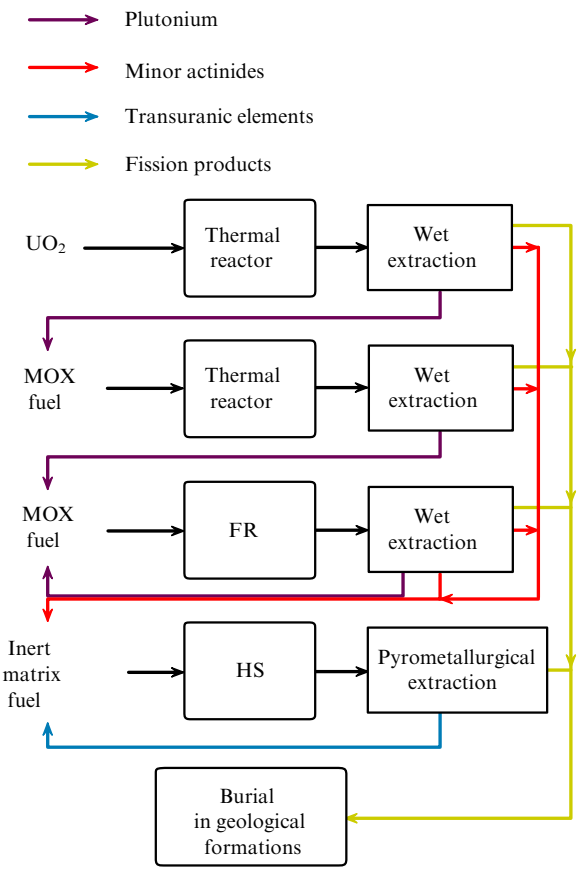

Figure 3. Example of NFC closure scheme involving MA burning in a hybrid system.

4. Hybrid systems with neutron sources based on nuclear spallation

At present, hybrid systems with neutron sources based on nuclear spallation (we shall use the established abbreviation ADS — accelerator-driven system) are studied the most. The main ADS components include a proton accelerator, a neutron-producing target, and a subcritical nuclear assembly. The cooling system and the system generating electricity are essentially the same as the respective systems of FRs and thermal reactors.

The generation of neutrons in a nuclear target is due to nuclear spallation reactions. In ADSs, this process is initiated by high-energy protons, $E_p > 200$ MeV. Here, the number of secondary neutrons in the nuclear spallation reaction depends both on the target material and geometry and on the incident beam energy. According to Ref. [15], the phenomenological formula describing the efficiency Y of neutron generation by a proton beam (determined by the number of neutrons per proton) in the case of a target of nonfissionable heavy elements (for example, lead or tungsten) has the form

$$Y = (W - 120)(A + 20) \times 10^{-4}\,, \qquad (2)$$

where W is the incident proton energy [MeV], and A is the relative atomic mass of the target nucleus. As is seen from formula (2), with enhancement of the proton beam energy the neutron generation efficiency per W of the beam power asymptotically approaches the value of $(A + 20) \times 10^9/1.6$ (Fig. 4). For this reason, enhancement of the proton energy to a level above ≈ 1 GeV makes no sense within the framework of the problem of neutron generation.

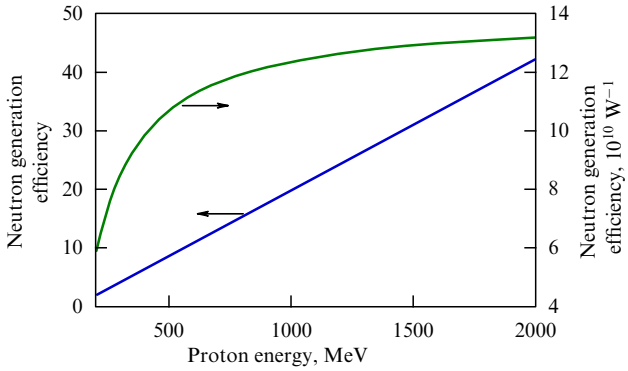

Figure 4. Dependence of neutron generation efficiency in a lead target by a proton accelerator. The dependence presented was calculated per proton and per W of the accelerator beam power.

The neutrons ejected from the source are fast and their energy spectrum has a maximum in the energy region of 1–2 MeV, while the neutron flux is nonzero in the energy range right up to the incident proton energy value. The generated neutrons are further brought into the subcritical nuclear assembly, where reactions take place with the fuel.

Requirements for the ADS accelerator, generally speaking, reduce to providing the necessary values of the proton current and energy, as well as the stability of the proton beam. For example, the project-demonstration of ADS technology MYRRHA (Multi-purpose hYbrid Research Reactor for High-tech Applications) at the Belgian Center of nuclear research (SCK/CEN) [16] implies the use of a proton beam with a current of 4 mA and energy of 600 MeV for an HS with a thermal power of 50–100 MW with a maximum admissible frequency of long (over 3 s) beam trips inferior to 0.1 such events per day [17]. For comparison, the operating linear accelerator SNS (Spallation Neutron Source) of the Oak Ridge National Laboratory (ORNL) in the USA produces a proton beam with an energy of 1 GeV and mean power of 1.4 MW [18]. Here, the frequency of long beam trips at SNS is by two-three orders of magnitude higher than the maximum admissible value for the MYRRHA project [19]. The EFIT system (see Section 4) will require the development of an accelerator producing a beam with a current of 20 mA and energy of 800 MeV at a frequency of long beam trips of less than three per year [10]. The rigid requirements for the beam stability are explained by thermocycling in elements of the ADS construction, which originates owing to beam trips or oscillations of its power and leads to a reduction of the service life period of the system elements. Besides, long beam trips may result in the necessity of terminating the reactor operation and initiating restarting procedures. The latter circumstance is especially important when the ADS is applied for the generation of electricity.

The requirements for the proton beam power are determined by the necessary thermal power of the reactor and by the neutron multiplication factor of the subcritical nuclear assembly. The proton beam current can be estimated if one knows the thermal power P_{th} of the subcritical assembly, the neutron multiplication factor[9] k_{sub}^{acc}, the mean number of neutrons $\bar{\nu}_{fis}$ emitted per fission act, and the fission

[9] The neutron multiplication factor k_{sub}^{acc} must, generally speaking, take into account the difference between the source neutron energy spectrum and the energy spectrum of fission neutrons of the subcritical assembly.

energy E_{fis}:

$$I_{\text{beam}} = P_{\text{th}} \frac{(1 - k_{\text{sub}}^{\text{acc}})\,\bar{\nu}_{\text{fis}}}{k_{\text{sub}}^{\text{acc}}} \frac{e}{Y(E_{\text{p}}, A)\,E_{\text{fis}}}\,, \qquad (3)$$

where e is the electron charge, and $Y(E_{\text{p}}, A)$ is the neutron generation efficiency calculated by formula (2). In formula (3) $k_{\text{sub}}^{\text{acc}}/[(1 - k_{\text{sub}}^{\text{acc}})\,\bar{\nu}_{\text{fis}}]$ is the number of fission acts initiated by a single neutron from the source. Choosing characteristic values of $P_{\text{th}} = 1$ GW, $k_{\text{sub}}^{\text{acc}} = 0.97$, $E_{\text{fis}} \approx 200$ MeV, $\bar{\nu}_{\text{fis}} \approx 2.5$, $E_{\text{p}} = 1$ GeV, and $Y \approx 20$, we obtain a proton beam current $I = 19$ mA and the respective power of the accelerator beam equal to 19 MW.

Within the framework of the problem of creating a neutron source for ADS, the generation of a continuous proton beam is considered with the aid of cyclotrons or linear accelerators (LINACs). Both technologies have demonstrated the capability of creating devices exhibiting beam power and energy close to the ones required for demonstration projects. An example of a powerful cyclotron is the proton accelerator at PSI (Paul Scherrer Institute) in Switzerland; of the powerful LINACs, one can single out the LANSCE (Los Alamos Neutron Science CEnter) accelerator at the Los Alamos National Laboratory (LANL), USA, and SNS (Fig. 5). Nevertheless, the use of LINACs is assumed in most of the long-term ADS projects. This relates to the fact that large beam currents can be attained taking advantage of linear accelerators. In linear accelerators with continuous proton beam generation, currents of the order of 100 mA are to be achieved at a final particle energy of 1 GeV, while in cyclotrons with the same final energy the intended beam current limit is about one tenth that amount [20, 21]. For devices-demonstrators of ADS technologies, the beam power provided by cyclotrons is sufficient; however, for devices with a thermal power of $\sim 500 - 1000$ MW, LINACs will be required.

To estimate the continuous proton beam generation efficiency in a LINAC with a proton energy of order 1 GeV, one can take advantage of the formula given in Ref. [20]:

$$P_{\text{grid}} = 1.9 P_{\text{beam}} + P_{\text{aux}}\,, \qquad (4)$$

where P_{grid} is the power consumed by the accelerator 'from the wall outlet', P_{beam} is the proton beam power, and $P_{\text{aux}} \approx 27$ MW represents the power losses independent of the beam current. The proportionality factor relating the beam power and the electric power consumed from the electrical supply network involves the AC to DC conversion efficiency in the power supply units (0.97), the efficiency (0.67) of high-frequency radiation generation by clystrons, as well as a 10% loss of radiation in the waveguide, and additional 10% losses due to unaccounted factors. We will need formula (4) in Section 6 for estimating the neutron generation efficiencies by different HS sources.

At present, accelerator-driven devices are the most thoroughly investigated class of hybrid systems; we mean not only theoretical studies but also experimental programs. Table 3 lists installations that are associated with studies of the physics and technology of ADSs either owing to the specific line of investigation or to device parameters.

As an example of ADS, we shall consider the European Facility for Industrial-scale Transmutation (EFIT) developed as an burner reactor of minor actinides within the framework of the EUROpean Research Programme for the TRANSmutation of High-Level Nuclear Waste in an Accelerator-Driven System (EUROTRANS). The EFIT system can be termed an

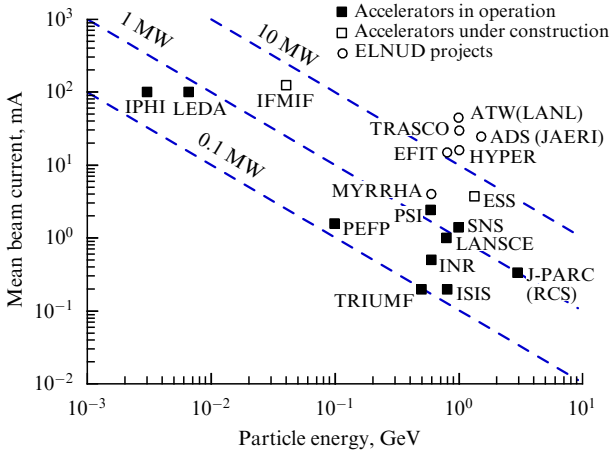

Figure 5. Mean beam current and energy in accelerators under construction and in operation and proton beam parameters necessary for different ADS projects: IPHI — Injector of Protons for High-Intensity beams; LEDA — Low-Energy Demonstration Accelerator; IFMIF — International Fusion Materials Irradiation Facility; TRASCO — from Italian: TRAsmutazione SCOrie; ATW — Accelerator Transmutation of Waste; ADS (JAERI) — Accelerator-Driven System (Japan Atomic Energy Research Institute); HYPER — HYbrid Power Extraction Reactor; ESS — European Spallation Source; PEFP — Proton Engineering Frontier Project, INR — Institute for Nuclear Research of RAS; J-PARC (RCS) — Japan Proton Accelerator Research Complex (Rapid Cycling Synchrotron), and TRIUMF — TRI-University Meson Facility, (Based on data from Refs [10, 16, 22–33].

Table 3. Experimental programs for studying ADS physics*

Title of experiment	Institution, country	Purpose
MEGAPIE	PSI, Switzerland	Technology adjustment of liquid-metal (Pb-Bi) target generating neutrons
SNS	ORNL, USA	Pulsed neutron source with LINAC and mercury target generating neutrons for studies based on neutron scattering
LEDA	LANL, USA	Proton accelerator with continuous beam generation (6.7 MeV, 100 mA) intended for demonstration and investigation of beam generation and of the first stage of beam acceleration in a high-current LINAC
Yalina	JIENR, Belarus	Investigation of parameters of a subcritical nuclear assembly with an external neutron source, validation of numerical models, adjustment of methods for diagnostics and control of a subcritical assembly
Venus-1	CIAE, China	
GUINEVERE	SCK/CEN, Belgium	
MUSE-4	CEA Cadarache, France	

* MEGAPIE — MEGAwatt PIlot Experiment; JIENR — Joint Institute of Energy and Nuclear Research 'Sosny'; CIAE — China Institute of Atomic Energy; GUINEVERE — Generator of Uninterrupted Intense NEutrons at the lead VEnus REactor; MUSE-4 — from French MUltiplication par Source Externe, and CEA — from French: Commissariat à l'Energie Atomique.

industrial-experimental burner reactor. In a certain sense, the role of EFIT in HSs based on nuclear spallation reactions is similar to the role of BN-600 in fast neutron reactors. In accordance with the EUROTRANS program, two essentially different versions of the system, described in Refs [10, 11], have been prepared. The difference between the versions lies in the different types of proton targets and heat carriers used in the subcritical nuclear ADS. As the main version, a system with a lead heat carrier and target generating neutrons (for convenience, we shall denote it as Pb-EFIT) is under consideration. The back up version is a system with a gas (He) heat carrier and a solid tungsten target for the proton beam — He-EFIT.

The rated thermal power of the system described amounts to 400 MW. The neutron source makes use of a proton accelerator with a beam current of 15–20 mA and proton energy of 800 MeV.

Both systems are intended for an NFC closure scheme involving maximization of the burnup rate of minor actinides in ADS (see Fig. 3). In this case, all the actinides of the fuel spent in EFIT are extracted jointly in the recovery process. On the one hand, this leads to the equilibrium content of plutonium isotopes in the fuel equal to $\mathrm{Pu}/(\mathrm{Pu}+\mathrm{MA}) \approx 40\%$. On the other hand, such an approach is favorable from the point of view of the nonproliferation policy. The MA burning up rate in the EFIT system amounts to 42 kg $(\mathrm{TW}^{(\mathrm{t})}\,\mathrm{h})^{-1}$. If the EFIT core were loaded only with minor actinides, it would be possible to achieve a high rate of MA elimination, but this would require continuous extraction of plutonium from the spent fuel of the system.

A liquid-metal lead target is used in Pb-EFIT, which is connected directly to the beam line. The target temperature conditions are sustained by a proton beam scanning the target surface in a direction perpendicular to the motion of the lead and by the most rapid possible circulation of the metal through the nuclear spallation zone (the circulation velocity of lead is limited to the value of $2\ \mathrm{m\ s^{-1}}$; otherwise, the target service lifetime will be reduced owing to corrosion). As a result, the highest and lowest target temperatures amount to 520 °C and 420 °C, respectively.

The proton target in the He-EFIT system has nothing in common with its analog in Pb-EFIT. For neutron generation in He-EFIT, a set of solid tungsten rods is used, cooled by helium, arranged perpendicularly to the beam propagation direction. The target construction requires utilization of a steel beam window for physical separation of the beam line and the target zone. The window is cooled with the aid of an independent cooling contour. The cooling contours of the blanket and of the target are also separated, and the gas pressure in them amounts to 70×10^5 and 14×10^5 Pa, respectively. The maximum power density released at the target reaches $3 \times 10^5\ \mathrm{W\ l^{-1}}$.

5. Subcritical hybrid systems with thermonuclear neutron sources

Another HS version concerns a system with a thermonuclear neutron source. Neutrons are produced in the source as a result of nuclear fusion reactions taking place in high-temperature plasma. As a rule, designs of neutron sources for HS rely on the deuterium–tritium (D–T) fusion reaction, since, although the problem of producing tritium does not exist in projects based on the D–D reaction, the intensity of reactions in the case of the same source parameters is about two orders of magnitude lower. It should be noted that most projects consider magnetic confinement of plasma in stationary conditions. We shall deal precisely with such projects, although, in principle, other approaches are also possible, such as those based on inertial confinement of plasma and pulsed neutron generation (project LIFE — Laser Inertial Fusion-Fission Energy [34]). The proposed projects have been widely publicized at international conferences and workshops [35, 36]. The system diversity is extremely broad here, since practically each system has its own neutron source configuration. Most of the projects are based on tokamaks, while the alternatives considered are stellarators and magnetic mirrors.

In the case of HSs with thermonuclear neutron sources, it is possible to single out a number of peculiarities. First, when neutron generation is due to the D–T fusion reaction, the tritium breeding in the system is required. Second, if the magnetic plasma confinement in the source is assumed, a serious problem consists in the magnetohydrodynamic (MHD) pressure drop due to the flow of molten salts or of a liquid-metal coolant in the magnetic field. It is also necessary for such systems to use materials with a relative permeability $\mu \approx 1$.

In considering tritium breeding in an HS, it is necessary to take into account various losses during the production and recirculation of tritium in the system, decays of nuclei, and the possibility of other HSs with thermonuclear neutron sources being put into operation. For this reason, the tritium breeding factor should reach a value of 1.05–1.2 atoms per fusion reaction [37]. Practically all the methods of tritium breeding for hybrid or thermonuclear reactors presume the employment of neutron reactions involving lithium isotopes:

$$^6\mathrm{Li} + \mathrm{n} \rightarrow {}^4\mathrm{He} + \mathrm{T}\,,$$
$$^7\mathrm{Li} + \mathrm{n} \rightarrow {}^4\mathrm{He} + \mathrm{T} + \mathrm{n}\,.$$

It should be noted that the reaction with ^{6}Li has a large cross section in the region of interaction energies lower than 1 MeV, and the reaction with ^{7}Li exhibits a threshold character ($E_{\mathrm{interaction}} > 3.84$ MeV). Lithium can be used for producing tritium within the lead–lithium eutectic, FLiBe or FLiNaBe molten salts, or in the form of lithium ceramics (Li_4SiO_4, Li_2TiO_3, Li_2O). The last method is envisaged in the project of the International Thermonuclear Experimental Reactor (ITER).

Another peculiarity of an HS with a thermonuclear neutron source is the MHD pressure drop emerging due to the flow of conducting material (for example, of the liquid-metal heat carrier of a subcritical assembly) across the magnetic field lines. In the SABR (Sodium Advanced Burner Reactor) project (see Section 5.1) making use of a sodium heat carrier, the calculated MHD pressure drop amounted to 68 MPa, which would lead to the necessity of applying an additional 0.85 GW of pumping power, comparable to the electric power of the installation. In the concrete case dealt with, this problem was proposed to be resolved by covering the surfaces of the fuel rods and of the subassemblies with a layer of the $LiNbO_3$ insulator, which is accompanied by a corresponding decrease in the MHD pressure drop to 2.5×10^{-6} Pa [38]. We note that the problem of a high MHD pressure drop does not arise, when the heat carrier used has a low conductivity, like helium or CO_2, or when the heat carrier flows predominantly along the magnetic field lines.

On the other hand, certain ADS problems will, most likely, be revealed in HSs with thermonuclear neutron sources, such as the problem of neutron generation stability. At present, all thermonuclear experimental devices operate in the mode of single pulses, although the pulse lengths of large tokamaks do exceed the time required for the plasma parameters to reach stationary values. Therefore, the issue of the frequency and duration of plasma disruptions and of the respective neutron generation disruptions in an HS remains open. Low-frequency plasma oscillations that can lead to modulation of the neutron flux and respective oscillations of the energy release in a subcritical assembly are also related to the issue of neutron generation stability. On the basis of requirements for ADS neutron sources (see Section 4), one can assume oscillations of frequencies below 10 Hz to be dangerous.

By analogy with formula (3), it is possible to introduce a relationship between the thermonuclear reaction power in a neutron source, P_{fus}, and the thermal power of a subcritical nuclear assembly, P_{th}:

$$P_{\text{fus}} = P_{\text{th}} \frac{(1 - k_{\text{sub}}^{\text{fus}})\,\bar{\nu}_{\text{fis}}}{k_{\text{sub}}^{\text{fus}}} \frac{E_{\text{fus}}}{E_{\text{fis}}}\,, \tag{5}$$

where E_{fus} is the energy released in the thermonuclear reaction, and $k_{\text{sub}}^{\text{fus}}$ is the neutron multiplication factor in an HS with a thermonuclear neutron source. Making use of the parameter values presented in Section 4 for the estimation of the proton beam current by formula (3) and assuming the D–T fusion reaction ($E_{\text{fus}} = 17.6$ MeV) to be used in the neutron source, we obtain an estimate for the power of thermonuclear reactions, $P_{\text{fus}} \approx 7$ MW, necessary for achieving a power of 1 GW in a subcritical system with $k_{\text{sub}}^{\text{fus}} = 0.97$.

It is necessary to make an important comment concerning the neutron multiplication factor in an HS with a thermonuclear neutron source and ADS. Even in the case of absolutely identical subcritical assemblies and spatial shapes of the neutron fluxes from the sources, one has $k_{\text{sub}}^{\text{acc}} \neq k_{\text{sub}}^{\text{fus}}$. The $\bar{\nu}_{\text{fis}}$ values also differ. This is related to the different energy spectra of neutrons from the sources and, as a consequence, the mean interaction cross sections with matter of neutrons from the respective sources differing from each other. A comparison of the properties of a subcritical system with a Pb–Bi heat carrier was performed in Ref. [39] with different neutron sources, but for identical assembly parameters. The neutron sources differed in the emitted neutron energy spectrum. In one case, an accelerator-driven source was used, and in another, a source based on D–T fusion reaction. The ratio of multiplication factors amounted to $2(k_{\text{sub}}^{\text{fus}} - k_{\text{sub}}^{\text{acc}})/(k_{\text{sub}}^{\text{fus}} + k_{\text{sub}}^{\text{acc}}) \approx 0.028$ for $k_{\text{sub}}^{\text{fus}} = 0.972$, $k_{\text{sub}}^{\text{acc}} = 0.945$. In this case, a significant deviation of the multiplication factors from each other is explained by the difference between the cross sections of (n, 2n) threshold reactions in lead and bismuth.

5.1 Hybrid systems with tokamak neutron sources

At present, tokamaks are considered the basis for creating thermonuclear fusion reactors for the production of electric power. At one of the largest tokamaks, JET (Joint European Torus), the power of thermonuclear reactions achieved in transient modes (below 1 s) was 16 MW, while in quasistationary conditions (with a pulse length of 5 s) it was about 4 MW with 'plasma' efficiencies of thermonuclear reactions $Q_{\text{plasma}} = P_{\text{fus}}/P_{\text{in}} = 0.62$ and 0.18, respectively, where P_{in} is the power captured in the plasma [10] [40]. Investigations necessary to complete the physical database for a tokamak-based reactor are to be performed at ITER [42], the construction of which is presently under way. The main goals of the ITER project are to demonstrate the quasistationary mode of plasma confinement during a pulse longer than 2000 s with $Q_{\text{plasma}} \approx 5$, and to achieve $Q_{\text{plasma}} \geqslant 10$ in a mode with a relatively short pulse longer than 400 s and a total power of thermonuclear reactions [11] of 500 MW [43]. From the point of view of the obtained power of thermonuclear reactions and the values of Q_{plasma}, tokamaks are doubtless the leaders; therefore, tokamaks give rise to the highest interest as candidates for the role of NSs for HS burners.

A significant disadvantage of tokamaks lies in high thermal and neutron loads on the first wall and the divertor. According to Ref. [44], the phenomenological load limit on the tokamak first wall amounts to 0.2 MW m^{-2}. When this limit was exceeded in experiments at TFTR (Tokamak Fusion Test Reactor), disruption of the plasma parameters occurred [45]. It must be taken into account that peak loads on the tokamak wall may be significantly higher. Thus, for example, during the development of plasma boundary instabilities (Edge Localized Mode, ELM) and during the plasma column disruption, the peak power may reach 10 GW with characteristic instability times of 0.5–5 ms. This leads to a rapid degradation of the neutron source first wall in the hybrid system. To resolve this problem, a proposal was made to introduce into the plasma periphery lithium admixtures, which provide energy absorption and its further reemission, which will aid in weakening the shock load [46].

At present, SABR (Subcritical Advanced Burner Reactor) can be singled out as an example of the well-developed HS burner project with a neutron source based on the 'classical' tokamak [38]. In SABR, a subcritical assembly with a liquid-metal (sodium) coolant and fuel composed of a mixture of MA and plutonium is to be applied. The neutron source is a tokamak facility with parameters close to the ITER parameters. Figure 6 shows a basic layout of the SABR installation. The plasma ring is placed inside a chamber of rectangular cross section (3.8 m high, the minimal and maximal radii are 2.8 and 5.0 m, respectively). The circular core surrounds the plasma from outside (with a minimal radius of 5.0 m, thickness of 0.6 m, and height of 3.2 m). The plasma and core are surrounded by a lithium blanket, reflector, and neutron shielding, which are situated inside superconducting magnetic coils. A comparison of the neutron source characteristics of SABR and ITER is presented in Table 4.

The SABR project is intended for joint burning of plutonium and minor actinides of the spent fuel of thermal reactors. The subcritical assembly uses metallic fuel with the following weight parts of elements: Zr — 40%, Am — 10%, Np — 10%, and Pu — 40%. As the main construction

[10] Note that the presented 'plasma' efficiency differs from the 'engineering' efficiency determined as $Q_{\text{eng}} = P_{\text{fus}}/P_{\text{grid}}$, where P_{grid} is the power of the electricity supply network necessary for the magnetic system supply, the plasma heating system, etc. In the case of the JET tokamak, a larger part of electric power is consumed by the magnetic system (up to 700 MW) [41] and Q_{eng} does not exceed several percent even in short-pulse experiments.

[11] In ITER, the use of superconducting magnets is assumed, which will essentially reduce the consumption of electric power by the system; therefore, the predicted engineering efficiency of thermonuclear reactions $Q_{\text{eng}} > 1$.

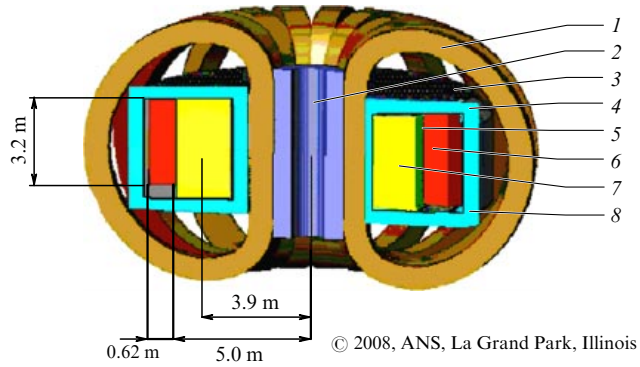

Figure 6. Schematic layout of SABR installation [38]: *1* — coils of a toroidal field, *2* — central solenoid, *3* — vacuum chamber, *4* — lithium blanket and neutron shield, *5* — first wall, *6* — core, *7* — plasma, and *8* — reflector and neutron shielding. This figure is published by courtesy of the authors of Ref. [38] and of the American Nuclear Society, La Grand Park, Illinois.

Table 4. Parameters of the SABR [38] neutron sources and ITER [43].

Parameter	SABR	ITER
Major radius, m	3.5	6.2
Magnetic field, T	5.9	5.3
Plasma current, MA	8 – 10	15
Power of fusion reaction, MW	up to 500	500
Q_{plasma}	3.2	$\geqslant 10$
Mean neutron load on the wall, MW m^{-2}	1	0.57

material for the core, utilization is proposed of oxide dispersion strengthened alloy MA957. The fuel burnup depth, like the exposure time, is limited by the radiation resistance of the fuel rod cladding, and for the limit damage level of 200 dpa chosen in the project it should amount to about 250 GW day t^{-1}.

It is also necessary to mention NS projects designed on the basis of spherical tokamaks, a peculiarity of which is the small aspect ratio R/a, where R is the radius from the system axis to the center of the plasma bunch, and a is the plasma radius. An important feature of spherical tokamaks is the possibility of achieving a high relative plasma pressure β (the ratio of the plasma pressure to the pressure of the magnetic field). From an engineering point of view, an increase in β permits weakening the magnetic field necessary for confinement of plasma with given parameters. The plasma stability is determined by the Troyon parameter, or the normalized β parameter: $\beta_{\text{N}} = \beta/[I/(aB)]$, where I is the current in the plasma, and B is the toroidal field. For classical tokamaks, the Troyon parameter is limited to the value of $\beta_{\text{N}} \approx 3-5$, while the relative plasma pressure $\beta < 10\%$. However, in the experimental spherical tokamak NSTX (National Spherical Torus eXperiment) (USA) β amounts to 40%. NS projects based on spherical tokamaks are considered, for example, in Refs [47, 48]; their characteristic parameters are presented in Table 5. The NS compact size complicates arrangement of the neutron shielding of superconducting magnets. Therefore, both projects are oriented toward employing copper coils for the magnets. The TIN-ST project is directed toward small dimensions and low electric power consumption: the total

Table 5. Comparison of parameters of SABR, CFNS, and TIN-ST projects.

Parameter	SABR [38]	CFNS* [47]	TIN-ST** [48]
Major radius, m	3.75	1.35	0.47
Aspect ratio	3.4	1.8	1.74
Magnetic field at the center of a plasma bunch, T	5.9	2.9	1.35
Power of fusion reaction, MW	up to 500	100	1 – 7.5***
Q_{plasma}	3	2	0.07 – 0.5***
β, %	≈ 3	15 – 18	≈ 60
β_{N}	2.5	2 – 3	1.7 – 4.9

* Compact Fusion Neutron Source.
** Thermonuclear neutron source (TNS) on the basis of a spherical tokamak (ST).
*** Beam-plasma mode [48].

consumption does not exceed 50 MW, while the power for plasma heating is not more than 15 MW.

Notice that in the case of HSs with NSs built around tokamaks, quite significant share of thermonuclear neutrons is lost in vein. For example, only 39% of the thermonuclear neutrons are utilized in the fuel core of the SABR. A larger part of the remaining neutrons take part in the production of tritium in the lithium blanket. Enhancement of the utilization factor of D–T neutrons could, in principle, permit obtaining comparable neutron fluxes in the active zone of the hybrid at a lower thermonuclear reaction power in the NS. In the case of 100% utilization of the D–T neutrons in SABR, the total power of thermonuclear reactions could be reduced by a factor of 2.5.

5.2 Systems with thermonuclear magnetic mirror neutron sources

Open traps [39, 49–53] are applied as NSs in a number of HS projects. All the projects considered with NSs based on magnetic mirrors imply the generation of thermonuclear neutrons by high-energy (fast) ions, produced either by intense atomic beams or by the introduction of microwave radiation at the cyclotron rotation frequency of ions [ion-cyclotron resonance (ICR) heating]. The main task of the 'thermal' background plasma consists in MHD stabilization of the fast ions.

A functional diagram of an HS with a neutron source based on a magnetic mirror is displayed in Fig. 7. Depending on the NS specific features, there are two possible ways of arranging a subcritical assembly with respect to the neutron source. The first corresponds to the case when neutron emission varies weakly within the central part of the facility and starts to decrease sharply only at its edges — near mirror coils. In this case, the nuclear assembly is extended along the entire length of the trap, as proposed, e.g., in Ref. [50]. The second version corresponds to the case of high-energy beams being injected and captured by the plasma and slowing down without significant angular scattering [39]. In this situation, 'turning point regions' appear on two sides of the facility center, within which the majority of fast ions are reflected from a rising magnetic field. In these regions, the density of fast ions and the rate of thermonuclear reactions are maximum; therefore, it is expedient to arrange subcritical assemblies around the turning point regions. However, in

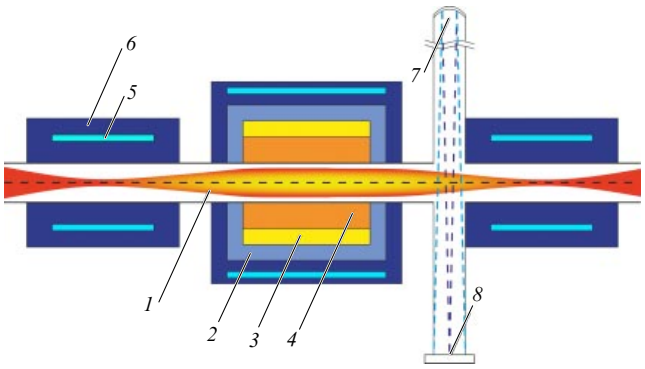

Figure 7. Schematic diagram of an axisymmetric HS with a neutron source based on an open trap: *1* — plasma, *2* — reflector, *3* — lithium blanket, *4* — core, *5* — magnetic coils, *6* — neutron shielding, *7* — injector of atoms, and *8* — beam receiver.

both of these cases, shielding of the heating injectors or antennas from thermonuclear neutrons has to be implemented.

Hybrids designed by involving magnetic mirrors have the following advantages over systems based on tokamaks.

• The construction of magnetic mirrors implies that the cylindrical subcritical assembly is arranged in a more convenient manner around the working chamber of the trap.

• The utilization efficiency of thermonuclear neutrons inside the core may reach 90–95%.

• No disruptions or thermal overloading of the source first wall occur in magnetic mirrors.

• In a source based on magnetic mirrors, it is possible to realize a plasma confinement mode with a value of $\beta \lesssim 1$.

From a physical point of view, the main disadvantage of magnetic mirrors consists in large longitudinal losses of thermal plasma. For this reason, confinement times and plasma temperatures in modern magnetic mirrors are significantly smaller than corresponding values in tokamaks, while the efficiency of thermonuclear reactions does not exceed $Q_{\text{plasma}} \sim 10^{-2}$. However, in the case of a trap involving gas-dynamic confinement, there is a simple way to improve longitudinal confinement. With increasing the length of the device, the number of particles in the trap increases in proportion to its length, while the power of longitudinal losses is limited by gas-dynamic quantities. Thus, in long magnetic mirrors it is possible to obtain high confinement times: the value of $Q_{\text{plasma}} \sim 1$ can be achieved for a length of the device of about 1 km. It should be noted that not even a single project has been realized in the past 30 years in constructing traps of the open type, which is due to tokamaks having already demonstrated plasma parameters closer to the ignition ones by the end of the 1980s.

Parameters of NSs based on magnetic mirrors are listed in Table 6. An NS project designed around a gas-dynamic trap (GDT) was considered in Refs [51, 52]. The NS is an axisymmetric device, in which plasma is heated by atomic beams. The length of the device is relatively small; therefore, the parameter Q_{plasma} has a value far from unity. A critical parameter for such a system is the electron temperature which determines the lifetime of fast ions. An essential issue, also, is MHD stabilization of plasma. In the projects proposed, the method of 'vortex confinement' is applied [54], which is quite simple in realization and does not require significant energy consumption. As an alternative, classical methods reported in

Table 6. Parameters of NSs based on open traps

Parameter \ Traps	NS-GDT [52]	NS-GDT [51]	SFLM [50]
Length of confinement region, m	16	16	25
Plasma radius in central cross section, cm	10	10	40
Magnetic field in central cross section, T	1	1	1.25–2
Mirror ratio	15	15	4
Power of fusion reaction, MW	6	15	≈ 10
Q_{plasma}	≈ 0.1	0.3	> 0.15
Electron temperature, keV	0.5	3	> 0.5

Ref. [55] can be considered, which consist in optimization of the longitudinal profiles of pressure and of the curvature of magnetic force lines. It should be noted that the physical principles of an NS based on GDT have been investigated quite thoroughly, and the parameters of the planned NS are not very far from the values achieved experimentally [56].

In the open-trap project with straight force lines (Straight Field Line Mirror concept, SFLM) [50], the problem of MHD stabilization was resolved in an essentially different way. The creators of the SFLM concept propose abandoning axial symmetry — a quadrupole magnetic field is applied, which provides plasma confinement in a configuration with the minimum $|B|$ on the axis of the device. In such an approach, the existence of thermal plasma is only necessary for the capture of atomic beams (if they are used) and, possibly, for stabilization with respect to kinetic instabilities. Heating of the ions may be achieved by two methods, which can be applied simultaneously: with the aid of ICR heating, and by the injection of atomic beams. ICR heating can be additionally applied for the improvement of fast ion confinement [57]. This circumstance can turn out to be important, since the mirror ratio (i.e., the ratio of the magnetic field in the mirror to the field in the central cross section) is small. Notice that the SFLM project requires a more detailed justification; this especially concerns the scheme of ICR heating and its influence on plasma confinement.

6. Competitive advantages of hybrid systems

The competitive ability of hybrid systems is not, generally speaking, determined by the cost of individual reactors, but by the cost of electricity generation within the scheme of the cycle closure, when the condition of total transmutation of transuranic elements is fulfilled. As noted in Section 3, the schemes of NFC closure with burning of plutonium (see NFC closure schemes 2–4 in Table 2) ensure approximately equal costs of electric power both in the case of HS utilization and without it (with the exception of the scheme involving the burning up of all transuranic elements in the HS). Therefore, it must be acknowledged that conventional FRs are quite capable of resolving the problem of burning up transuranic elements without applying subcritical hybrid systems. Here, the availability of technologies related to FRs has reached a stage still inaccessible to technologies making use of ADS or, more so, hybrids based on thermonuclear fusion. On the whole, it can be said that further prospects of the development of hybrid systems will depend quite much on the rate of large-

scale installation of FRs and on the termination of the operation of thermal nuclear reactors.

As to a comparison of the costs of devices pertaining to different HS classes, it is too early to perform such comparison owing to the relative immaturity of HS technologies. One might, however, compare neutron production at the source normalized to 1 W of electric power consumption in the cases of accelerator and thermonuclear neutron sources, which, as will be seen below, differ significantly. Here, it is naturally necessary to bare in mind that this parameter is far from the only one, so a thorough comparison of ADS and hybrid systems with thermonuclear neutron sources represents the subject of a separate investigation.

Using formulas (2), (4), the possibility arises to calculate the neutron generation efficiency of an accelerator-driven source:

$$S_{\rm acc} = \frac{Y(E_{\rm p}, A)\, P_{\rm beam}}{P_{\rm grid}\, E_{\rm p}}\,, \qquad (6)$$

where $S_{\rm acc}$ is the neutron generation efficiency of an accelerator-driven source normalized to 1 W of electric power from the network, $Y(E_{\rm p}, A)$ is the neutron generation efficiency by a target in accordance with formula (2), $P_{\rm beam}$ is the proton beam power, and $P_{\rm grid}$ is the power supplied by the network to the neutron source. Thus, $S \sim 3 \times 10^{10}$ neutrons per W for the neutron source of the Pb-EFIT system [10].

In an HS with the thermonuclear NS, the generation of neutrons, which is totally determined by the efficiency of thermonuclear reactions in the source, can be expressed as

$$S_{\rm fus} = \frac{P_{\rm fus}}{P_{\rm grid}\, E_{\rm fus}}\,, \qquad (7)$$

where $E_{\rm fus}$ is the thermonuclear reaction energy, and $P_{\rm fus}$ is the power of thermonuclear reactions inside the source. If an NS involving the D–T fusion reaction is used, one can arrive at the estimate $S_{\rm fus} \approx 3.55 \times 10^{11} P_{\rm fus}/P_{\rm grid}$.

A comparison of the neutron production efficiencies with the aid of accelerator and thermonuclear neutron sources, respectively, is presented in Fig. 8. Referring to formulas (6), (7) and Fig. 8, already at relatively small $Q_{\rm eng} \approx 0.1-0.2$, certainly accessible for installations at the ITER level, a D–T neutron source produces neutrons with a higher efficiency.

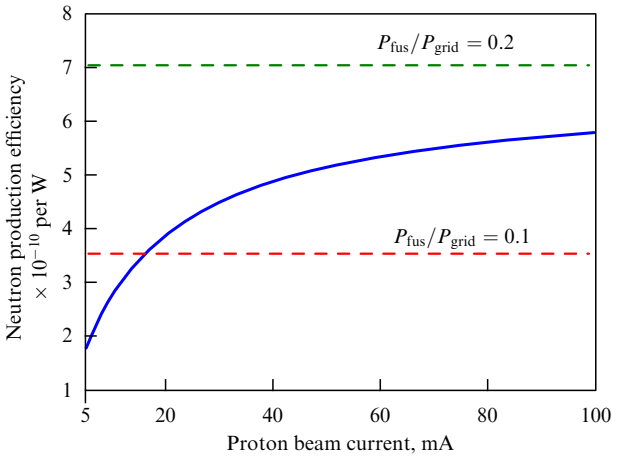

Figure 8. Efficiency of neutron production calculated for 1 W of power consumption by accelerator-driven neutron source with proton energy of 1 GeV versus beam current. Dashed straight lines indicate neutron production efficiencies for a D–T thermonuclear neutron source with $P_{\rm fus}/P_{\rm grid} = 0.1$ and 0.2, respectively.

Table 7. Main parameters of SABR, Pb-EFIT, and He-EFIT HSs.

Characteristic \ Installation	SABR [38]	Pb-EFIT [10]	He-EFIT [11]
Type of a neutron source	Thermonuclear neutron source, $Q_{\rm plasma} = 3.2$	800 MeV, 14-mA beam, liquid-metal target (Pb)	800 MeV, 15-mA beam, solid W target
$k_{\rm eff}$	0.82 – 0.89	0.97	0.97
$\Delta k_{\rm eff}$ during fuel exposure time, 10^{-3}%	7000	600	≈ 400
Rated thermal power, GW	3	0.4	0.4
Neutron generation efficiency, W^{-1}	$\approx 3.5\times10^{11}$ *	2.8×10^{10} *	2.6×10^{10} *
Source power in neutrons	1.8×10^{19} – 1.8×10^{20}	3.1×10^{17} *	3.1×10^{17} *
MA/(MA + Pu) from conventional reactors, %	33.3	100	100
Burnup, GW day t^{-1}	250	78	≈ 120 *
Geometric utilization of source neutrons, %	39	?**	≈ 75

* Estimation by authors of the present article.
** No data found.

For the reader's convenience, Table 7 presents a summary of the main parameters of HSs dealt with in this article. As seen from Table 7, thermonuclear NSs are superior to accelerator NSs in neutron generation efficiency and, in principle, they are capable of providing a greater neutron flux. Consequently, thermonuclear neutron sources will be able to provide the necessary neutron generation in high-power systems exhibiting, at the same time, a low neutron multiplication factor $k_{\rm eff}$.

7. Conclusion

The results presented in this article permit us to draw several important conclusions concerning the state of affairs and of prospects for developing the HS burners of transuranic elements in spent nuclear fuel.

Actually, the problem of burning transuranic elements can be resolved on its own, without making use of HSs, only with the aid of fast neutron reactors, although this is only possible if the relative number of FRs in the reactor stock is sufficiently high. Burning up of all transuranic elements in HSs makes sense only if the technology of critical FRs is totally abandoned. In the short-term perspective, the burning of minor actinides in HSs may become important. On the one hand, this option permits realizing the competitive advantage of HS burners, consisting in the possibility of practically achieving the limiting MA burning rate. On the other hand, this permits NFC closure without extensive FR utilization. In the long term, the need for HSs burners will decrease as the relative number of FRs in the reactor stock increases.

While hybrid systems resolve the reactor safety problems peculiar to FRs by processing minor actinides, they create a number of problems typical only for their class. None of the neutron source technologies for HS burners has hitherto demonstrated the entire set of required parameters. It still

remains to be demonstrated that accelerator neutron sources have achieved the necessary beam power and stability. But, here, ADS projects have been investigated more thoroughly than HS burners based on thermonuclear NSs: a number of experimental programs have been implemented and device-demonstrators of the technology are to be created. Modern thermonuclear devices operate in the regime of single pulses and still exhibit an extremely low engineering efficiency of thermonuclear reactions. In the ideal case, however, they are capable of providing a higher neutron generation efficiency and a larger neutron flux than spallation NSs depending on nuclear fission for their operation.

Acknowledgment
This work received financial support from the Ministry of Education and Science of the Russian Federation (RFMEF161914X0003).

References

1. Apse V A et al. *Fiziko-Tekhnicheskie Osnovy Sovremennoi Atomnoi Energetiki*: *Perspektivy i Ekologicheskie Aspekty* (Physical-Technical Fundamentals of Modern Nuclear Power Engineering: Prospects and Ecological Aspects) (Dolgoprudny: Intellekt, 2014)
2. Shmelev A N et al. *Atom. Energy* **73** 963 (1992); *Atom. Energ.* **73** 450 (1992)
3. Wallenius J *Nucl. Eng. Technol.* **44** 199 (2012)
4. IAEA, Evaluated Nuclear Data File, https://www-nds.iaea.org/exfor/endf.htm
5. Wallenius J, Eriksson M *Nucl. Technol.* **152** 367 (2005)
6. Hoffman E A, Yang W S, Hill R N "Preliminary core design studies for the Advanced Burner Reactor over a wide range of conversion ratios", ANL Report ANL-AFCI-177 (Argonne, Ill.: Argonne National Laboratory, 2006); http://www.ipd.anl.gov/anl pubs/2008/05/61507.pdf
7. Messaoudi N, Tommasi J *Nucl. Technol.* **137** 84 (2002)
8. Ando Y, Nishihara K, Takano H *J. Nucl. Sci. Technol.* **37** 924 (2000)
9. "Status of minor actinide fuel development", IAEA Nuclear Energy Series technical report NF-T-4.6 (Vienna: IAEA, 2009); http://www-pub.iaea.org/MTCD/Publications/PDF/Pub1415_web.pdf
10. Mansani L et al. *Nucl. Technol.* **180** 241 (2012)
11. Pignatel J F et al. *Nucl. Technol.* **180** 264 (2012)
12. "Accelerator-Driven Systems (ADS) and Fast Reactors (FR) in advanced nuclear fuel cycle. A comparative study", OECD/NEA Report (Paris: OECD Publ., 2002); https://www.oecd-nea.org/ndd/reports/2002/nea3109-ads.pdf
13. "Advanced nuclear fuel cycles and radioactive waste management", OECD/NEA Report 5990 (Paris: OECD Publ., 2006); https://www.oecd-nea.org/ndd/pubs/2006/5990-advanced-nfc-rwm.pdf
14. Salvatores M, Palmiotti G *Prog. Part. Nucl. Phys.* **66** 144 (2011)
15. Polozov S M, Fertman A D *Atom. Energy* **113** 192 (2013); *Atom. Energ.* **113** (3) 155 (2012)
16. MYRRHA: Multi-purpose hybrid research reactor for high-tech applications, http://myrrha.sckcen.be/en
17. Vandeplassche D et al., in *Proc. IPAC 2011 Conf., San Sebastian, Spain, September 2011*, p. 2718; http://accelconf.web.cern.ch/AccelConf/IPAC2011/papers/weps090.pdf
18. "SNS Parameters List", SNS 100000000–PL0001–R13, (ORNL, 2005); http://neutrons.ornl.gov/media/pubs/pdf/sns_parameters_list_june05.pdf
19. Vandeplassche D, Romão L M, in *Proc. IPAC 2012 Conf., New Orleans, USA, May 2012* (2012) 6; http://ipnwww.in2p3.fr/MAX/images/stories/downloads/SCK-CEN_IPAC12.pdf
20. "Accelerator and spallation target technologies for ADS applications (A status report)", OECD/NEA Report 5421 (Paris: OECD Publ., 2005); https://www.oecd-nea.org/science/docs/pubs/nea5421-accelerator.pdf
21. Kapchinskii I M *Sov. Phys. Usp.* **23** 835 (1980); *Usp. Fiz. Nauk* **132** 639 (1980)
22. Wangler T P, "Reliable–Linac design for accelerator-driven subcritical reactor systems", LANL Report LA–UR–02–6684 (Los Alamos, NM: Los Alamos National Laboratory, 2002); http://library.lanl.gov/cgi-bin/getfile?00937251.pdf
23. Kravchuk L V, in *Proc. of the XXI Russian Particle Accelerators Conf., RuPAC, 2008, Zvenigorod, Russia*, p. 137
24. Pottin B et al., in *Proc. of LINAC 2012, Tel-Aviv, Israel*, p. 921
25. Wei J et al., in *Proc. HB 2006*, p. 39
26. Tsujimoto K et al. *J. Nucl. Sci. Technol.* **41** 21 (2004)
27. Suzuki H, in *Proc. of APAC 2004, Gyeongju, Korea*, p. 499
28. Callaway N T et al., in *Proc. of the 1997 Particle Accelerator Conf.* Vol. 1 (New York: IEEE, 1998) p. 1165
29. Vernon S H, in *Proc. of the 2001 Particle Accelerator Conf.* Vol. 5 (New York: IEEE, 2001) p. 3296
30. Kwon H J et al., in *Proc. of LINAC 2012, Tel-Aviv, Israel* p. 422
31. Grillenberger J et al., in *Proc. of Cyclotrons, 2013, Vancouver, BC, Canada*, p. 37
32. Park W S et al. *Nucl. Eng. Design* **199** 155 (2000)
33. Dutto G, in *Trudy XIII Mezhdunarod. Konf. po Uskoritelyam Chastits Vysokikh Energii, Novosibirsk, 7–11 Avgusta 1986* (Proc. of the XIII Intern. Conf. on Accelerators of High-Energy Particles, Novosibirsk, 7–11 August 1986) Vol. 1 (Exec. Ed. A N Skrinsky) (Novosibirsk: Nauka, 1987) p. 270
34. Moses E I et al. *Fusion Sci. Technol.* **56** 547 (2008)
35. *Third Fusion-Fission Hybrids Workshop, East-West Science Center of the Univ. of Maryland, USA, 2009*
36. *Workshop on Fusion for Neutrons and Sub-Critical Nuclear Fission, Villa Monastero, Italy, 2011*
37. Abdou M A "Tritium breeding in fusion reactors", ANL/FPP/TM-165 (1982); in *Nuclear Data for Science and Technology. Proc. of the Intern. Conf., 6–10 September 1982* (Ed. K H Böckhoff) (Brussels: ECSC, EEC, 1983) p. 293
38. Stacey W M et al. *Nucl. Technol.* **162** 53 (2008)
39. Noack K et al. *Ann. Nucl. Energy* **35** 1216 (2008)
40. Jacquinot J and the JET team *Plasma Phys. Control. Fusion* **41** A13 (1999)
41. http://www.efda.org/jet
42. http://www.iter.org/
43. Aymar R, Barabaschi P, Shimomura Y *Plasma Phys. Control. Fusion* **44** 519 (2002)
44. Mirnov S *AIP Conf. Proc.* **1442** 15 (2012)
45. Johnson D W et al. *Plasma Phys. Control. Fusion* **37** A69 (1995)
46. Mansfield D K et al. *Phys. Plasmas* **3** 1892 (1996)
47. Kotschenreuther M et al. *Fusion Eng. Design* **84** 83 (2009)
48. Kuteev B V et al. *Plasma Phys. Rep.* **36** 281 (2010); *Fiz. Plazmy* **36** 307 (2010)
49. Moir R W et al. "Axisymmetric magnetic mirror fusion-fission hybrid", Report LLNL-TR-484071 (2011); *Fusion Sci. Technol.* **61** 206 (2012)
50. Agren O et al. *AIP Conf. Proc.* **1442** 173 (2012)
51. Anikeev A V, Dagan R, Fischer U *Fusion Sci. Technol.* **59** (1T) 162 (2011)
52. Yurov D V et al. *Fusion Eng. Design* **87** 1684 (2012)
53. Noack K et al. *Ann. Nucl. Energy* **38** 578 (2011)
54. Beklemishev A D et al. *Fusion Sci. Technol.* **57** 351 (2010)
55. Rosenbluth M N, Longmire C L *Ann. Physics* **1** 120 (1957)
56. Ivanov A A, Prikhodko V V *Plasma Phys. Control. Fusion* **55** 063001 (2013)
57. Agren O, Savenko N *Phys. Plasmas* **12** 022506 (2005)